

Search for a Standard Model Higgs boson in the $H \rightarrow \gamma\gamma$ channel with the ATLAS detector *

LEONARDO CARMINATI
ON BEHALF OF THE ATLAS COLLABORATION

Università degli Studi e sez. INFN di Milano

The search of a Standard Model Higgs boson in the two photons channel with the ATLAS detector is reviewed with a particular emphasis on the expected detector performance. The results of the inclusive analysis on the most recent samples of full simulated events are reported. The overall discovery potential in this channel is finally updated including a discussion on NLO corrections.

PACS numbers: 14.80.Bn

1. Introduction

The Standard Model Higgs Boson decay into two photons is a promising discovery channel in the $115 < m_H < 140$ GeV mass range at the LHC. The mentioned mass range is also favoured by the global fit on electroweak variables which sets a 95% confidence level upper limit to $m_H < 189$ GeV. The Higgs decay into two photons is a rare process with a branching ratio times cross section of the order of only 50 fb. The final state consists of two high- p_T photons ($p_T \sim 50$ GeV) with an invariant mass compatible with the Higgs boson mass. Despite the simple signature it's one of the most challenging channel for the detector: excellent energy and angular resolutions are needed to observe the narrow mass peak above the $\gamma\gamma$ QCD continuum which has a typical cross sections ~ 125 fb/GeV (NLO for $M_H = 120$ and after kinematical cuts and photon efficiency). In addition a powerful particle identification capability is required to reject the background coming from jet-jet and γ -jet events in which one or both jets are misidentified as photons whose cross sections are many order of magnitude larger than the signal.

* Presented at "Physics at LHC 2006", Cracow 3-8 July 2006



The analysis has been completely reviewed with respect to the results presented in the in the ATLAS Physics TDR ([1]) using updated GEANT 3 ([2]) based detector simulations, newer versions of PYTHIA ([6]) and the available NLO generators.

2. Main experimental aspects of the analysis

2.1. Photon identification and jet rejection

The identification of isolated high transverse momentum photons ($p_T > 25$ GeV) is essential in the search for the Higgs in the $\gamma\gamma$ channel. In order to reduce the jet-jet and γ -jet background to a level below that of the irreducible $\gamma\gamma$ continuum a single jet rejection factor of ~ 5000 is required. In order to separate photons from jets, discriminating variables are defined based on both calorimeter and inner tracking system. Cuts on these variables are developed to keep high photons efficiency ($\sim 80\%$) even in the presence of pile-up. The offline photon/jet separation procedure consists mainly of the following steps:

1. calorimeter information is used to select events containing high E_T electromagnetic showers. The fine grained first compartment of the electromagnetic calorimeter allows a further rejection of π^0 induced showers.
2. inner detector information is used to improve the results using a track isolation algorithm.

The ATLAS performance in the gamma/jet separation has been tested on a large set of full simulated dijet QCD events (more details in [4]). After all cuts a jet rejection factor of ~ 5000 in both high (10^{34} cm⁻² s⁻¹) and low ($2 \cdot 10^{33}$ cm⁻² s⁻¹) luminosity conditions has been obtained keeping an overall photon efficiency of about 80 % as reported in fig. (1). Different jet rejections factor has been obtained for quark and gluon initiated jets: for $p_T > 25$ GeV the rejection after the isolation cut is 2880 ± 190 for quark initiated jets and 20650 ± 2370 for gluon jets. This is due to the lower probability of fragmentation of gluons to π^0 carrying a large fraction of the original parton momentum: the impact of this difference on the Higgs discovery potential is discussed in section 4.

2.2. Photons calibration and reconstruction

The expected S/\sqrt{B} in this channel is proportional to the inverse of the square root of the mass resolution of the Higgs peak. As in the interesting mass range the Higgs width is negligible (a few MeV), the mass resolution is

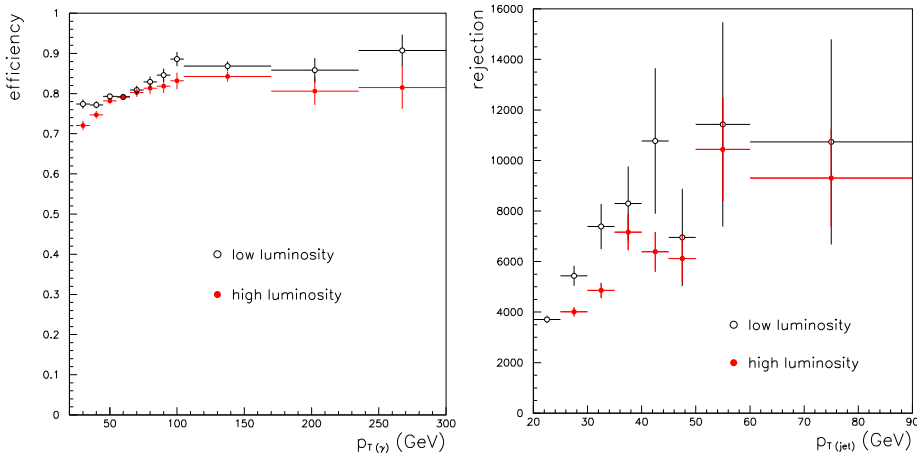


Fig. 1. Efficiency (left) and jet rejection (right) as a function of p_T at low and high luminosity including track isolation cut.

dominated by experimental resolution. This can be expressed as a function of the photon energy and position resolutions as:

$$\frac{\sigma_{M_H}}{M_H} = \frac{1}{2} \left[\frac{\sigma_{E_1}}{E_1} \oplus \frac{\sigma_{E_2}}{E_2} \oplus \frac{\sigma_\alpha}{\tan(\alpha/2)} \right], \quad (1)$$

where E_1 and E_2 are the energies of the two photons measured in the electromagnetic calorimeter and α is the angle between them. The calibration algorithm has been carefully optimized on GEANT 3 based simulations of the detector and the obtained results show that the requirements for the $H \rightarrow \gamma\gamma$ analysis can be generally fulfilled ([3]): the sampling term of the energy resolution can be kept at the level of 10%-15%/ \sqrt{E} and the non linearity has found to be of the order of a few permille in the required energy range. The resolution on the θ angle is of the order of 60 mrad/ \sqrt{E} while on ϕ position is 4-6 mrad/ \sqrt{E} also thanks to precise knowledge of the primary vertex in the transverse plane at the LHC.

In order to reduce the contribution of the angular term to the mass resolution (see eq. 1) the photon direction must be known with a good accuracy. Since at the LHC the z coordinate of the primary vertex will be known with a $\sigma_z = 5.6$ cm, a more accurate reconstruction of the primary vertex is required. As the two photons do not provide any charged track that can be reconstructed in the Inner Detector (unless they convert), the primary

vertex has to be determined from tracks produced with the Higgs boson. The presence of pileup is dangerous to the success of this technique so that this method is foreseen in the low luminosity phase. At high luminosity conditions it is more difficult to identify the Higgs primary vertex among the pileup vertices: in this case the stand-alone measurement of the γ direction provided by the electromagnetic calorimeter has to be used: a resolution on the z coordinate of the primary vertex of ~ 16 mm has been obtained in high luminosity conditions.

3. Analysis cuts and Higgs invariant mass reconstruction

In the standard inclusive analysis the following kinematical cuts are applied in order to optimize the signal significance:

1. The two photon candidates are required to have a transverse energy greater than 40 and 25 GeV respectively
2. Both photons are required to hit the electromagnetic calorimeter in the region $|\eta| < 2.5$
3. Three η regions have been excluded where the electromagnetic calorimeter response is not optimal: the gap between the two half barrels $|\eta| < 0.05$, the barrel-endcap transition region $1.37 < |\eta| < 1.52$ and the last part of the endcap outer wheel $2.37 < |\eta| < 2.5$.

An example of the invariant mass distributions of the two photons from a $M_h=120$ GeV Higgs decay is reported in figure 2. The mass resolutions determined from an asymmetric gaussian fit ($[-2\sigma, +3\sigma]$) on the mass peak for different Higgs are masses reported in table 1. In the following the *mass bin* will be defined as window of $\pm 1.4 \sigma$ around the central value.

M_H	120 GeV	130 GeV	140 GeV
$\sigma_{M_H} (2 \cdot 10^{33} \text{ cm}^{-2} \text{ s}^{-1})$	1.36	1.42	1.51
$\sigma_{M_H} (10^{34} \text{ cm}^{-2} \text{ s}^{-1})$	1.59	1.65	1.70

Table 1. Mass resolutions at low luminosity (Inner Detector primary vertex measurement with nominal 40 μm z-resolution included in the direction reconstruction algorithm) and high luminosity (electromagnetic calorimeter stand-alone direction reconstruction) for different Higgs boson masses.

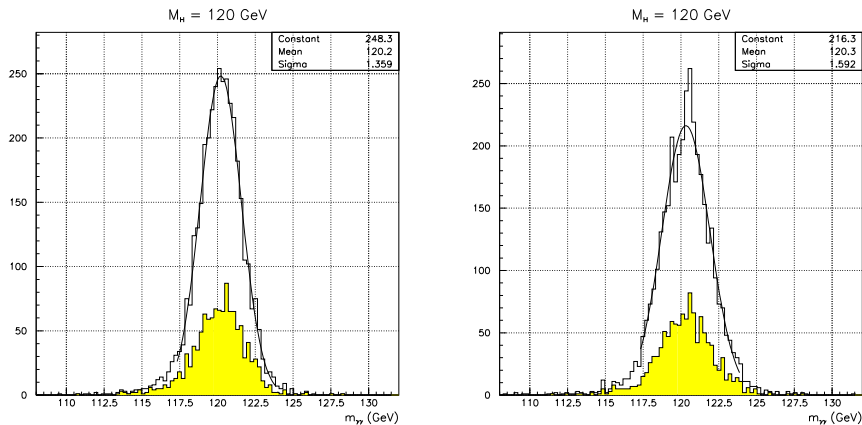


Fig. 2. Reconstructed two photons invariant mass for $H \rightarrow \gamma\gamma$ decay at low (left) and high luminosity (right). The yellow histograms represent events containing at least one converted photon.

4. ATLAS Higgs discovery potential in the $\gamma\gamma$ channel

4.1. Signal significance

The $H \rightarrow \gamma\gamma$ decay has been analyzed in the past ([1]) using LO calculation while NLO, NLL and sometimes NNLO calculation are now available for both signal and background so that the analysis can be revisited in a consistent way. Signal and background cross sections have been computed using different tools.

For what concerns the signal, ResBos ([5]) NLO Monte-Carlo generator for the gluon gluon fusion has been used. Higgs production by vector boson fusion was generated by Pythia 6.224 to which was added a P_T independent constant $K = \sigma_{NLO}/\sigma_{LO}$ factor from HiGlu ([7]). The transition from LO to NLO gives rise to a K factor of 1.8 for the dominant gluon-gluon fusion process and for the vector boson fusion. Additional Higgs production processes of quark fusion and associated production were generated by Pythia. The LO Pythia branching ratio into two photons has been corrected with the one obtained by HDecay ([8]).

Concerning the irreducible backgrounds ResBos was used to derive the NLO cross section: an increase of the order of 47 % with respect to the LO has been obtained.

The dominant contribution to the reducible background consists of jet-jet events which are dominated by gluon initiated jets which are easier to reject with respect to the quark initiated jets. On the contrary quark initiated jets are the dominant contribution to the γ -jet events. To take the NLO into ac-

count, a factor $K=\sigma_{NLO}/\sigma_{LO}=1.7$ ([9]) has been included for the reducible background. The numbers of expected signal and backgrounds events in the mass bins are reported in table 2.

M_H	120 GeV	130 GeV	140 GeV
Signal	815	758	610
Irr. Backg.	14100	11472	9552
jet-jet Backg.	603	553	483
γ-jet Backg.	3364	2843	2356
S/\sqrt{B} (30 fb ⁻¹)	6.06	6.22	5.48
S/\sqrt{B} (100 fb ⁻¹)	9.81	10.07	8.84

Table 2. Number of expected signal and backgrounds events in the mass bins at NLO for 30 fb⁻¹ of integrated luminosity. Statistical significances S/\sqrt{N} are reported in the case of 30 and 100 fb⁻¹ of integrated luminosity

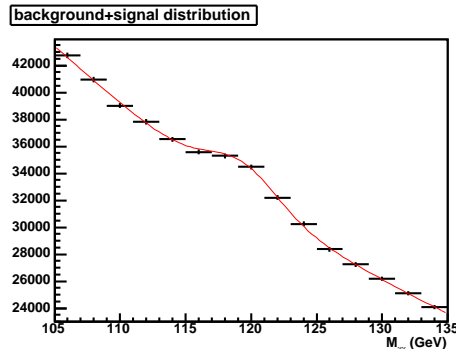


Fig. 3. Expected $H \rightarrow \gamma\gamma$ signal for a $M_H = 120$ GeV Higgs boson for 100 fb⁻¹ of integrated luminosity.

The statistical significance computed as a counting experiment as a function of the Higgs mass is reported in fig. 4 for 30 fb⁻¹ of integrated luminosity collected in low luminosity conditions and 100 fb⁻¹ of integrated luminosity collected in high luminosity conditions using both LO and NLO cross sections.

The discovery potential can be increased by $\sim 30\%$ using a likelihood technique ([10]) based on the shape of the distributions of some kinematical

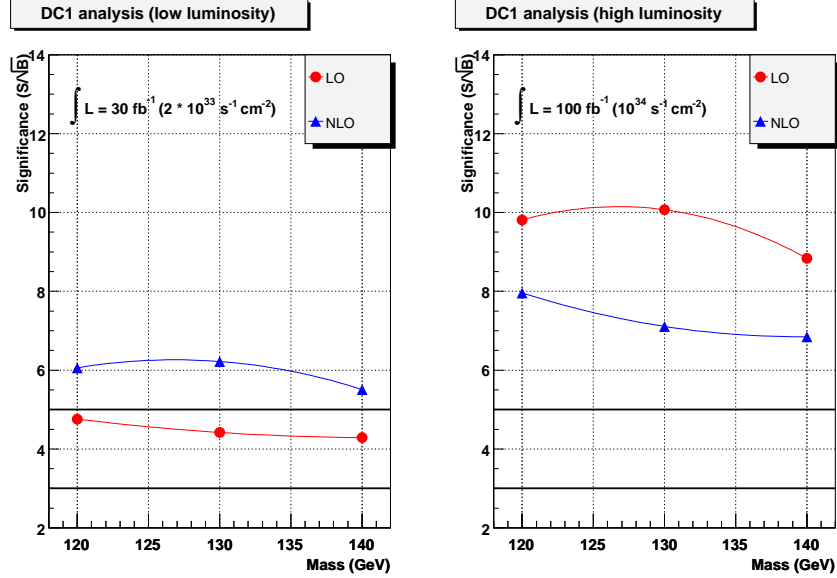


Fig. 4. statistical significance as a function of the Higgs mass for 30 fb^{-1} of integrated luminosity collected in low luminosity conditions ($2 \cdot 10^{33} \text{ cm}^{-2} \text{ s}^{-1}$) and 100 fb^{-1} of integrated luminosity collected in high luminosity conditions ($10^{34} \text{ cm}^{-2} \text{ s}^{-1}$) using both LO and NLO cross sections

variables. The most relevant inclusive variables are the transverse momentum of the photon pair and the angle in the center of mass of the two photons system between one photon and the center of mass velocity in the laboratory. NLO computations for signal and background are required to obtain a reliable prediction for these quantities.

4.2. Uncertainties on the signal significance

There are many uncertainties on the Higgs boson production cross section as well as on the background cross sections which have a direct consequence on the estimation of the ATLAS Higgs boson discovery potential. These uncertainties are mainly due to the parameterization of the PDF, the choice of renormalization and factorization scales, the order of perturbative development and the branching ratios. Assuming that the different contributions are uncorrelated an uncertainty of the order of 35 % has been estimated in the 100-140 GeV mass range. For what concerns the irreducible background an uncertainty of the order of 18 % has been determined taking into account the PDF uncertainty, the scale dependence and the photons isolation modelling. From previous studies ([11]) a factor of 3 uncertainty

on the reducible background has been assumed. Assuming that the different contributions are not correlated one can deduce uncertainty of 50 % on the predicted significance.

To quote the significances reported in table 2 a perfect knowledge of the average value of the background in the mass window is assumed. In reality the background normalization and shape will be determined on data from a fit on the sidebands of the mass distribution. This would reduce by $\sim 10\%$ the statistical significance by increasing the uncertainty on the background.

5. Conclusions

The ATLAS detector discovery potential of a Standard Model Higgs boson in the $H \rightarrow \gamma\gamma$ channel has been reviewed on most recent full detector simulation. The expected detector performance both in terms of photons reconstruction and identification capabilities generally fulfill the requirements, in agreement with previous studies. Thanks to the use of NLO prediction the expected discovery potential is enhanced by $\sim 50\%$ with respect to previous LO analysis ([1],[3]). Although the uncertainties are large, the ATLAS detector is expected to see a Higgs boson decay in the $\gamma\gamma$ channel with a statistical significance greater than 5 only with 30 fb $^{-1}$ of integrated luminosity. Less integrated luminosity could be enough by using likelihood techniques or combined H+0jet, H+1jet ([12]) and VBF ([13]) analyses which are now being addressed.

REFERENCES

- [1] The ATLAS Collaboration, CERN/LHCC/99-14/15 (1999).
- [2] S. Agostinelli et al., NIM A 506 (2003) 250-303,
- [3] M. Bettinelli et al., ATL-PHYS-PUB-2006-016
- [4] M. Escalier et al., ATLAS note ATL-PHYS-PUB-2005-018
- [5] C. Balazs and C.P. Yuan, Phys.Rev. D56 5558-5583 (1997), hep-ph/9704258
- [6] T. Sjostrand et al., Comput. Phys. Commun. 135 238-259(2001), hep-ph/0010017
- [7] M. Spira, hep-ph/9704258
- [8] A. Djouadi et al., Comput. Phys. Commun. 108 56-74(1998), hep-ph/9704448
- [9] T. Binoth et al., Eur.Phys.J.Direct C4 7 (2002), hep-ph/0203064
- [10] M. Escalier, CERN-THESIS-2005-023 (in french)
- [11] F. Gianotti, I. Vichou, ATLAS Note, ATL-PHYS-96-078
- [12] V. Zmushko, Atlas Note ATL-PHYS-2002-020
- [13] K. Cranmer et al., Atlas Note ATL-PHYS-2003-036